Vol 18 No 2, February 2009
1674-1056/2009/18(02)/0658-06

Chinese Physics B

© 2009 Chin. Phys. Soc.
and IOP Publishing Ltd

Pair interaction of bilayer-coated nanoscopic particles*

Zhang Qi-Yi(张启义)†

Department of Mathematics and Physics, Chongqing University of Science and Technology, Chongqing 401331, *China*

(Received 11 July 2008; revised manuscript received 9 August 2008)

The pair interaction between bilayer membrane-coated nanosized particles has been explored by using the self-consistent field (SCF) theory. The bilayer membranes are composed of amphiphilic polymers. For different system parameters, the pair-interaction free energies are obtained. Particular emphasis is placed on the analysis of a sequence of structural transformations of bilayers on spherical particles, which occur during their approaching processes. For different head fractions of amphiphiles, the asymmetrical morphologies between bilayers on two particles and the inverted micellar intermediates have been found in the membrane fusion pathway. These results can benefit the fabrication of vesicles as encapsulation vectors for drug and gene delivery.

Keywords: bilayer membrane, inverted micellar intermediates, nanoparticle, self-consistent field theory

PACC: 6125H, 8720, 8725D

1. Introduction

Bilayer membranes supported on solid substrates[1,2] are commonly used as cell-surface models because they can be applied to experiments in a broad range of cell membrane processes. Except the planar-supported membranes, the spherical-supported membranes (i.e. membranes on particles) offer some unique advantages for a range of applications. For example, the membrane-coated colloidal system has potential applications in monitoring molecular interactions on cell membrane surfaces,[3] by adjusting the lipid membrane composition and the pair interaction potential between the membrane-supporting silica beads. The system of bilayer-coated particle resembles the structure of vesicle with the solvents in the inner region of the closed structure replaced by particle. For convenience, we sometimes call this structure a 'vesicle' in the present article.

It is necessary to better understand the fundamental interactions between the coating membranes involved in these applications. The interaction between biological membranes is normally a process mediated by proteins, which may involve membrane fission and fusion. Fusion between pure lipid systems, i.e. spontaneous fusion, has a number of technological applications such as liposome based drug delivery[4,5] and the formation of supported lipid bilayer biosensors and other devices.[1] Interest in this subject also partially stems from cell-cell interactions that are dominant in many aspects of life. Hence, elucidating the physical mechanism of the vesicle interaction is central to understanding a wide range of biological phenomena. A number of theoretical models[6−10] and experimental researches[11−15] have proposed several membrane fusion mechanisms and suggested many fusion pathways. Here, this paper will focus on the morphological transformations of the bilayers during interaction process.

The main constituent of the bilayer membrane is amphiphile, which may be surfactant, lipid or block copolymer.[16] In recent years, cell-like vesicles made from purely synthetic block copolymers, polymersomes,[17] have become attractive and promising research objects because of their unique properties (thicker and stabler than any natural lipid membrane). The similarity in structure between the synthetic polymer vesicles[16,18] and cells provides an opportunity to use polymersomes as a model to explore membrane mediated processes, such as membrane fusion[12] and fission,[11] nonviral gene delivery[19] and packaging of DNA. Recently, a simple model of diblock copolymer in a solvent of homopolymer has been

*Project supported by the National Natural Science Foundation of China (Grant No 20804060).

†E-mail: qyzhang520@163.com

used to investigate the membrane fusion[20] and the biomimetic membranes hosting inclusions.[21,22]

For the theoretical method in this paper, the same coarse-grained membrane model[21,22] is used to study the pair interactions of 'vesicles' encapsulating nanoparticles, by reducing the inter-particle distance. The self-consistent field (SCF) technique can give structural information about the fusion between the coating bilayers, and the energies involved in the fusion process. Recent developments of experimental techniques such as optical[23−25] and magnetic[26] tweezers make it possible to trap, manipulate, and transfer biological objects. In a certain degree, the process of our theoretical model is similar to the phenomenon induced by mechanical force. This system is also expected to be particularly useful for studying inter-vesicle interactions. The encapsulated content within vesicles may be proteins[27] or nanoparticles.[28,29]

The rest of the present paper is organized as follows. The theoretical model and methodology are described in Section 2. The results are presented in Section 3. Conclusions are given in Section 4.

2. Theory

The SCF theory[30−35] has been detailed extensively elsewhere, so only a brief description of this technique is provided here in this paper. The incompressible system comprises n_a amphiphilic 'lipid' molecules, n_s solvent molecules and two solid spherical nanoparticles with the same radius R. Each of the amphiphiles is represented by a copolymer molecule containing N monomers with a head group (hydrophilic monomers (H)) connected to a tail group (hydrophobic monomers (T)). The fraction of head group in the amphiphile is denoted as f. Each of the solvents (S) is represented by a homopolymer molecule comprising N hydrophilic monomers only. All the monomers are determined based on a common number density ρ_0. The hydrophobic and hydrophilic monomers interact with a local repulsion of strength being χ, the Flory–Huggins parameter, and a choice $\chi N = 30$.[36]

The geometry of our two-dimensional model is illustrated in Fig.1. The system is placed in the xz plane. At the beginning of our calculation, two spherical particles with a distance d are pre-coated with two identical bilayers.[20] The distance is measured between the centres of the particles. Outside the closed bilayer are the solvent molecules.

The surface of the nanoparticle is impenetrable and hard. The total number density at position $\boldsymbol{r}$, $\phi_0(\boldsymbol{r})$, drops to zero at surface in a boundary region of width ε according to

$$\phi_0(\boldsymbol{r}) = \begin{cases} 0, & r \le R, \\ \dfrac{1}{2}\left\{1 - \cos\left(\dfrac{\pi(r-R)}{\varepsilon}\right)\right\}, & R \le r \le R+\varepsilon, \\ 1, & \text{else}, \end{cases} \tag{1}$$

where the value of ε is chosen to be much smaller than the value of R_g[37−39] the polymer radius of gyration.

The surface field H, which acts on the monomers close to the nanoparticle, is modelled as[38]

$$\frac{H(\boldsymbol{r})}{\chi N} = \begin{cases} \infty, & r \le R, \\ \Lambda\left\{1 + \cos\left(\dfrac{\pi(r-R)}{\varepsilon}\right)\right\}, & R \le r \le R+\varepsilon, \\ 0, & \text{else}, \end{cases} \tag{2}$$

where Λ controls the strength of the field at the nanoparticle surface. A negative value of Λ corresponds to a hydrophilic interaction, while a positive value indicates a hydrophobic interaction. Here, Λ is set to be -0.8 for a favourable adhesive interaction between the membrane and the particle.

In grand canonical ensemble,[20,40−42] the free-energy functional has the form

$$\begin{aligned}\frac{N\mathcal{F}}{\rho_0 k_{\mathrm{B}} T V} =& -\frac{1}{V}Q_{\mathrm{s}} - \frac{\exp(\mu/k_{\mathrm{B}}T)}{V}Q_{\mathrm{a}} \\ &+ \frac{1}{V}\int \mathrm{d}\boldsymbol{r}\chi N\left[\phi_{\mathrm{T}}(\boldsymbol{r})\phi_{\mathrm{H}}(\boldsymbol{r}) + \phi_{\mathrm{S}}(\boldsymbol{r})\phi_{\mathrm{T}}(\boldsymbol{r})\right] \\ &+ \frac{1}{V}\int \mathrm{d}\boldsymbol{r}H(\boldsymbol{r})\left[\phi_{\mathrm{H}}(\boldsymbol{r}) + \phi_{\mathrm{S}}(\boldsymbol{r}) - \phi_{\mathrm{T}}(\boldsymbol{r})\right] \\ &- \frac{1}{V}\int \mathrm{d}\boldsymbol{r}\left[\omega_{\mathrm{H}}(\boldsymbol{r})\phi_{\mathrm{H}}(\boldsymbol{r}) + \omega_{\mathrm{T}}(\boldsymbol{r})\phi_{\mathrm{T}}(\boldsymbol{r}) + \omega_{\mathrm{S}}(\boldsymbol{r})\phi_{\mathrm{S}}(\boldsymbol{r})\right] \\ &+ \frac{1}{V}\int \mathrm{d}\boldsymbol{r}\xi(\boldsymbol{r})\left[\phi_{\mathrm{H}}(\boldsymbol{r}) + \phi_{\mathrm{S}}(\boldsymbol{r}) + \phi_{\mathrm{T}}(\boldsymbol{r}) - \phi_0(\boldsymbol{r})\right]. \end{aligned} \tag{3}$$

Here V is the total volume of the system, and μ is the relative chemical potential of amphiphiles. Because of the assumed incompressibility constraint, there is only one independent chemical potential. The local volume fractions of the head and tail group of the amphiphiles are given by $\phi_{\mathrm{H}}(\boldsymbol{r})$ and $\phi_{\mathrm{T}}(\boldsymbol{r})$. Likewise, $\phi_{\mathrm{S}}(\boldsymbol{r})$ is the local concentration of solvents. $\omega_{\mathrm{H}}(\boldsymbol{r})$ is used to denote the value of the mean field felt by the head group at r, $\omega_{\mathrm{T}}(\boldsymbol{r})$ the field for tail group, and $\omega_{\mathrm{S}}(\boldsymbol{r})$ the field for solvents. The Q_{S} and Q_{a} are the single molecule partition functions of the solvents and amphiphiles subjected to the above fields. A Lagrange multiplier field $\xi(\boldsymbol{r})$ is introduced to enforce incompressibility.

Within the well-established SCF theory, the boundary conditions are needed. At the boundaries on the nanoparticles, the Dirichlet conditions are used, because of the hard particles and molecule cannot cross the boundaries. For the other four boundaries of our simulation box, the Neumann conditions are used.

3. Results and discussion

First, two equilibrated spherical 'vesicles' are created by artificially 'biased' structure[20−22,43] and located far enough from each other along the axis of approach (x axis), so that they do not feel each other. This is the starting configuration, which is taken to be a reference state. Each of them envelops a nanosized particle with the same radius $R = 1.0R_g$. Then, two particles are brought together sufficiently slowly so that the system is maintained in quasiequilibrium. At each given value of separation d, the free energy $\mathcal{F}(d)$ of the system and the concentration distribution of the 'vesicles' are calculated. For convenience, we consider the interaction free energy, $F(d)$,

$$F(d) = \mathcal{F}(d) - \mathcal{F}(\infty). \tag{8}$$

The chemical potential of the amphiphiles is fixed at $\mu/k_{\mathrm{B}}T = 4.25$. In the following, we investigate the variation of the architecture parameter f.

A typical case of interaction is illustrated in Fig.1 for parameter $f = 0.3$. The process of the two 'vesicles' approaching each other comprises two stages: the fusion of the two outer monolayers and the mergence of the two inner monolayers. Two completely isolated 'vesicles' (the state a1) each enveloping a nanoparticle eventually evolve into one 'vesicle' (the state a6) that entraps two particles into its interior.

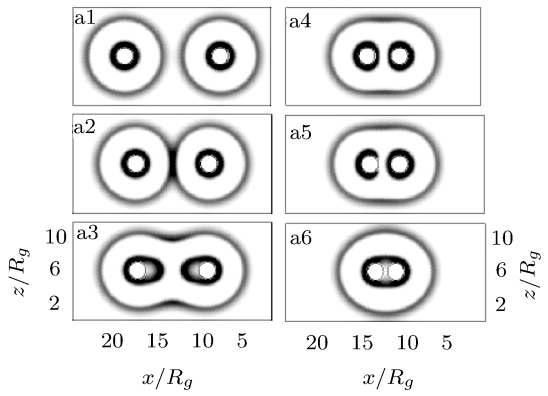


Fig.1. Density profiles of 'vesicles' for six different distances, showing that the distance is decreasing from a1 to a6, which correspond to the states marked by the solid circles in Fig.2(a). Only the head component is shown at each point. The head components are dark. Between the inner and the outer dark leaflets are tail segments. Outside the outer dark leaflets are solvent segments. The area enclosed by the small dark circle represents the nanoparticle. For convenience, all of the density distributions in the present paper obey the same rule: segment density decreasing is represented by different colours from black to white in a map.

The corresponding free energy of the system is shown in Fig.2(a). The two jumps in free energy

curve, i.e. from a2 to a3 and a4 to a5, correspond to the above two stages respectively. The two isolated noninteracting 'vesicles' are taken to be in the initial states (see a1). In the approaching process, first in Fig.1(a2), two 'vesicles' dragged by nanoparticles start to adhere to each other and a flattened contact forms between the 'vesicles' in which only the amphiphiles in the outer monolayers can intermix with each other. Then, two outer monolayers fuse into one monolayer with two symmetrical concaves (see a3), whereas the two inner monolayers remain independent. When the distance is reduced further, two inner leaflets are squeezed together (see a4). In the present system parameters, an interesting phenomenon appears that the monolayer on one of the two particles is squeezed to lose its structural integrity (see a5), not as it was in a4. It loses the part between the two particles, while the monolayer enveloping the other particle almost remains its structural integrity without any deformation. From a3 to a6, the two concaves (see a3) in the newly formed outer monolayer disappear gradually, and the resulting outer monolayer is converted from elliptical shape (see a4 and a5) into nearly spherical shape (see a6). Especially in state a6, two 'vesicles' are merged into one integral 'vesicle'. The behaviour of the two aggregated particles in a6 resembles that of one entrapped particle in the interior of 'vesicle'. This is similar to the encapsulation of 12 nm Fe_3O_4 nanoparticles in vesicles.[28]

The spontaneous curvature of each of the monolayers in vesicle is an important factor in membrane fusion.[9] Here, the spherical nanoparticle provides a high curvature environment for the amphiphile molecules. The architectural parameter of the amphiphile, f, is especially sensitive to this type of confined environment. Hence, different values of f can give various interaction morphologies. Figures 2(b) and 2(c) show the plots of the interaction free energy for $f = 0.25$ and 0.2, respectively. The states labelled with b1,...,b7 and c1,...,c8 are presented in Figs.3 and 4 respectively.

All the three interaction potentials in Fig.2 show a similar trend of monotonic decrease as the separation between two particles reduces. The energy jumps in interaction potential curves correspond to different morphological transformations of the membranes. In Fig.2, the values of distance d, corresponding to the first jumps, i.e. from a2 to a3, b1 to b2 and c1 to c2, increase with a decrease in f. It means an easier fusion with a smaller value of f.[6] Firstly, this is because before fusion, the outer monolayer is less favourable to the amphiphiles with smaller values of f.[33] While, compared with the outer monolayer, the concave environment formed after fusion is more favourable to the amphiphiles with smaller values of f. Secondly, this phenomenon can also be proven from membrane morphologies of the states before ruptures of two outer monolayers, i.e. the states a2, b1 and c1. The intermediate state a2 is the formation of a thin amphiphile bridge (stalk) linking two outer monolayers. In the contact area, the amphiphiles of the two outer leaflets can intermix with each other, and so the two monolayers cannot be distinguished. This is favoured by the stalk hypothesis.[13] While the formation of pores in b1 and c1 is different from that in a2. In b1, the rupture occurs right after the contact of two outer monolayers; they do not form a bridging monolayer like a2 and two monolayers can be distinguished clearly in the contact zone. The two outer monolayers of the state c1 almost do not change, then the rupture occurs suddenly as compared with b1. These 'vesicle' fusions from the contact of the outer monolayers roughly accord with Brownian dynamics simulations in Ref.[9].

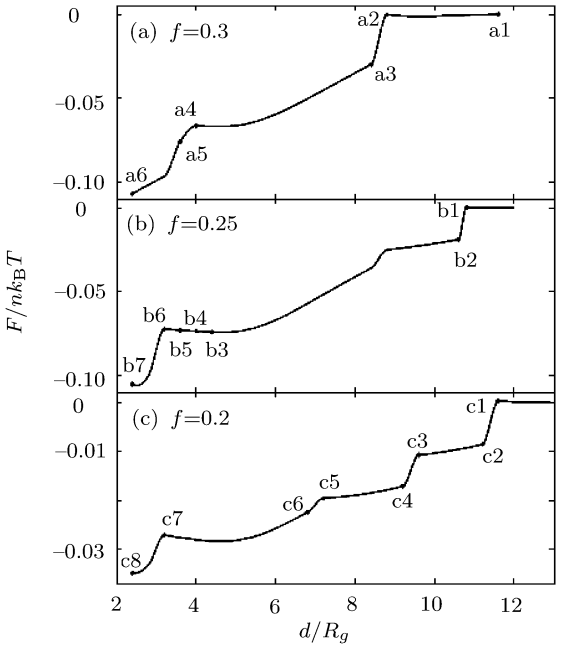


Fig.2. The interaction free energy, F/nk_BT, between two 'vesicles' encapsulating nanoparticles, as a function of separation d for various amphiphile architectures: $f = 0.3$ (a), 0.25 (b), and 0.2 (c). Different states are represented by solid circles labelled with a1...a6, b1...b7, and c1...c8, which are shown in Figs.1, 3 and 4 respectively.

Some very interesting findings appear in the second stage, i.e. right after the fusion of two outer

monolayers and just before the contact of two inner monolayers.

Figure 3 displays a sequence of images of bilayers enveloping nanoparticles for $f = 0.25$. From b4 to b6, the inner monolayers between two particles are squeezed heavily to rupture in their approaching directions. Two monolayers cannot coexist in the small space between two particles. So, the two inner monolayers compete with each other for their accommodations in this small area. From b4 to b5, this space is so narrow that it is only available for one monolayer. First in b4, the right inner monolayer is squeezed to lose a small piece in its approaching direction. It loses the structural integrity and the right particle contacts tail segments partially, whereas, the left inner monolayer remains its previous integral shape. The monolayer structures on the two particles are asymmetrical. Then, as the distance decreases in b5, the morphology of the right inner monolayer seems to be exchanged with that of the left one. The right monolayer resumes the integrated shape; while the left one loses a piece with the majority of the particles surrounded by head segments and the minority by the tail segments. In b6, as the space between two particles is reduced further, it accommodates less amphiphiles. Both particles release pieces of inner monolayers and they are exposed partially to tail segments. They resume symmetrical structures. The values of distance d for two, one, and no monolayer between two nanoparticles are approximately $4.4R_g$, $4R_g$, and $3.2R_g$, respectively, because the bilayer thickness is about $3.8R_g$. This phenomenon is mainly controlled by the value of f and also appears in other system parameters such as $\mu = 4.38k_{\rm B}T$ and $R = 1.5R_g$, which is checked in our calculations.

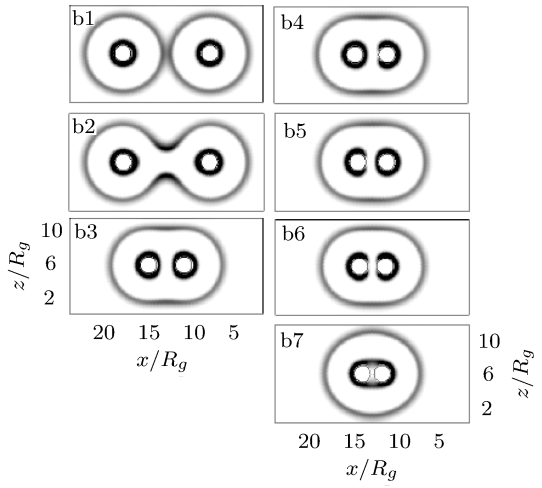


Fig.3. Density distributions of 'vesicles' for seven different distances. Distance is decreasing from b1 to b7, which correspond to the states marked by the solid circles in Fig.2(b).

With a smaller head fraction of amphiphile, for example $f = 0.2$, an inverted micellar intermediate[44−46] emerges, which is shown in Fig.4. Membrane-membrane interactions that can occur via inverted micellar intermediate in vesicle dispersions are illustrated in detail in Ref.[45]. Here, the formation of the inverted micelle is caused by the two concaves moving away from each other in order for the formation of nearly elliptical-shaped outer monolayer to reduce the interfacial energy, not by the close apposition of the two inner monolayers.[44,46] Compared with Fig.2(b), the corresponding interaction free energy in Fig.2(c) displays two jumps, i.e. from c3 to c4 and c5 to c6. In Fig.4, the two energy jumps correspond to the formation and the disappearance of the spherical inverted micelle between two inner monolayers, respectively. From c2 to c4, the inverted micelle grows larger and larger in size, until it reaches the largest size in c4; then from c4 to c6, it turns smaller and smaller until it completely disappears in c6. The following states from c7 to c8 are similar to those from b6 to b7.

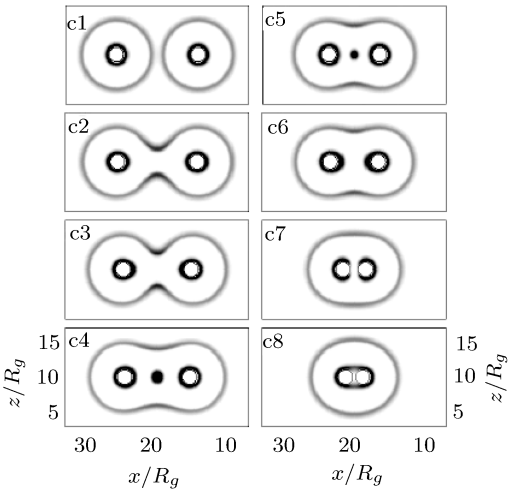


Fig.4. Density distributions of 'vesicles' for eight different distances. Distance is decreasing from c1 to c8, which correspond to the states marked by the solid circles in Fig.2(c).

4. Conclusions and remarks

In this work, the interaction potential between two bilayer-coated nanoparticles has been successfully probed by using the SCF theory. For different system

parameters, the interaction free energies are similar to each other, but the membrane structure evolutions may differ. Focusing on the bilayer transformations during the two nanoparticles approaching each other, this article gives the interaction process: two outer leaflets fuse, then two inner monolayers merge and develop into an integrity, which envelops the two particles into its interior. The two coated particles approaching process exhibits some very interesting results, including the inverted micelle structures and the asymmetrical morphologies of two inner monolayers on particles.

It is necessary for the successful fusion of two outer monolayers to overcome a small barrier. In our system, the fusion barriers are very small partly because of the smallness of the vesicle with high curvature, and the same polymerization of the amphiphile and the solvent molecules. The vesicles correspond to a diameter of $8.6R_g$. It is believed that the configurational property of the bilayer is mainly influenced by the value of f in this high curvature condition on the surface of the spherical particle. The chemical potential of the amphiphiles and the radius of the nanoparticle also have an influence on the configurational property of the bilayer, but do not provide any new morphology.

Our models have provided a detailed understanding of the physical processes involved in the interactions of membrane-coated particles, and given an insight into the structural evolution of the vesicle as it interacts with other vesicles. Such studies are also beneficial for understanding the process of the lysosome interaction with the interior component of cell and for designing the biomimetic vesicles to perform 'lifelike' functions. The vesicle fission induced by two nanoparticles will also give some interesting phenomena. These studies are underway currently.

References

[1] Sackmann E 1996 *Science* **271** 43
[2] Tanaka M and Sackmann E 2005 *Nature* **437** 656
[3] Baksh M M, Jaros M and Groves J T 2004 *Nature* **427** 139
[4] Dass C 2002 *Drug Delivery* **9** 169
[5] Lasic D 1998 *Trends Biotechnol.* **16** 307
[6] Smeijers A F, Markvoort A J, Pieterse K and Hilbers P A J 2006 *J. Phys. Chem.* B **110** 13212
[7] Noguchi H and Takasu M 2001 *J. Chem. Phys.* **115** 9547
[8] Stevens M J, Hoh J H and Woolf T B 2003 *Phys. Rev. Lett.* **91** 188102
[9] Noguchi H 2002 *J. Chem. Phys.* **117** 8130
[10] Markvoort A J, Smeijers A F, Pieterse K, van Santen R A and Hilbers P A J 2007 *J. Phys. Chem.* B **111** 5719
[11] Zhou Y F and Yan D Y 2005 *Angew. Chem. Int. Ed.* **44** 3223
[12] Zhou Y F and Yan D Y 2005 *J. Am. Chem. Soc.* **127** 10468
[13] Heuvingh J, Pincet F and Cribier S 2004 *Eur. Phys. J.* E **14** 269
[14] Yang L and Huang H W 2002 *Science* **297** 1877
[15] Haluska C K, Riske K A, Artzner V M, Lehn J M, Lipowsky R and Dimova R 2006 *Proc. Natl. Acad. Sci. USA* **103** 15841
[16] Discher D E and Eisenberg A 2002 *Science* **297** 967
[17] Discher B M, Won Y Y, Ege D S, Lee J C M, Bates F S, Discher D E and Hammer D A 1999 *Science* **284** 1143
[18] Luo L and Eisenberg A 2001 *Langmuir* **17** 6804
[19] Korobko A V, Backendorf C and Maarel J R C 2006 *J. Phys. Chem.* B **110** 14550
[20] Katsov K, MÄuller M and Schick M 2004 *Biophys. J.* **87** 3277
[21] Zhang Q Y and Ma Y Q 2006 *J. Chem. Phys.* **125** 164710
[22] Zhang Q Y and Ma Y Q 2006 *J. Phys. Chem.* B **110** 26279
[23] Fygenson D K, Marko J F and Libchaber A 1997 *Phys. Rev. Lett.* **79** 4497
[24] Li Q, Feng W L, Hu X M, Cao Q, Sha D G and Lin J M 2008 *Chin. Phys.* B **17** 726
[25] Xu S H, Li Y M, Lou L R and Sun Z W 2005 *Chin. Phys.* **14** 382
[26] Bausch A R, Ziemann F, Boulbitch A A, Jacobson K and Sackmann E 1998 *Biophys. J.* **75** 2038
[27] Harries D, Shaul A B and Szleifer I 2004 *J. Phys. Chem.* B **108** 1491
[28] Wijaya A and Schifferli K H 2007 *Langmuir* **23** 9546
[29] Smith K A, Jasnow D and Balazs A C 2007 *J. Chem. Phys.* **127** 084703
[30] Matsen M W and Schick M 1994 *Phys. Rev. Lett.* **72** 2660
[31] Fredrickson G H, Ganesan V and Drolet F 2002 *Macromolecules* **35** 16
[32] Shi A C, Noolandi J and Desai R C 1996 *Macromolecules* **29** 6487
[33] Matsen M W 2002 *J. Phys.: Condens. Matter* **14** R21
[34] Rasmussen K Ø and Kalosakas G 2002 *J. Polym. Sci.* Part B: *Polym. Phys.* **40** 1777
[35] Guo K K, Qiu F, Zhang H D and Yang Y L 2006 *Acta Phys. Sin.* **55** 155 (in Chinese)
[36] Matsen M W 2003 *Macromolecules* **36** 9647
[37] Matsen M W 1997 *J. Chem. Phys.* **106** 7781
[38] Lee J Y, Shou Z and Balazs A C 2003 *Phys. Rev. Lett.* **91** 136103
[39] Müller M and Binder K 2005 *J. Phys.: Condens. Matter* **17** S333
[40] Thompson R B and Matsen M W 2000 *J. Chem. Phys.* **112** 6863
[41] Matsen M W 1999 *J. Chem. Phys.* **110** 4658
[42] Matsen M W 1995 *Phys. Rev. Lett.* **74** 4225
[43] Lee J Y, Shou Z and Balazs A C 2003 *Phys. Rev. Lett.* **91** 136103
[44] Siegel D P 1993 *Biophys. J.* **65** 2124
[45] Siegel D P 1986 *Biophys. J.* **49** 1171
[46] Katsov K, Müller M and Schick M 2006 *Biophys. J.* **90** 915